Geophysical Prospecting, 1996, 44, 153–173

High-speed photography of the bubble generated by an airgun[1]

Jan Langhammer[2] and Martin Landrø[3]

Abstract

High-speed photography has been used visually to study the shape, surface, turbulence and behaviour of an underwater oscillating bubble generated by an airgun. The source was a BOLT airgun with a chamber volume of 1.6 cu.in., placed in a 0.85 m^3 tank at 0.5 m depth. Near-field signatures were also recorded in order to compare the instant photographs of the oscillating bubble with the pressure field recorded about 25 cm from the gun. Estimations of the bubble-wall velocity and bubble radius estimated from high-speed film sequences are also presented, and are compared with modelled results. The deviation between the modelled and measured bubble radii was at most 9%. In order to check the capacity for transmission of light through the bubble, a concentrated laser beam was used as illumination. We found that the air bubble is a strong scattering medium of laser light, hence the bubble is opaque.

Introduction

Due to its reliability and signature repeatability, the airgun has been the most common marine seismic source for the last two decades. There exist different types of airgun (conventional four-port gun, GI gun, Sleeve gun, etc.) based on different principles.

One of the main problems in understanding the pressure signature generated by an airgun is the lack of energy-dissipation mechanisms in the modelling theory. Compared to measured signatures, the synthetic signatures are underdamped. This problem has been considered by Ziolkowski (1970, 1982, 1990), Dragoset (paper presented at Offshore Technology Conference, Houston, Texas, 1984), Laws, Hatton and Haartsen (1990) and Landrø and Sollie (1992). Energy-loss mechanisms such as turbulence, heat transfer, mass transfer and viscosity have been introduced in the modelling. It has been assumed that both heat and mass transfer across the bubble wall occur via evaporation and condensation of water vapour (Ziolkowsi 1982). Ziolkowski and Metselaar (1984) and Ziolkowski (1990)

[1]Received October 1994, revision accepted June 1995.
[2]PGS Reservoir Services, PO Box 354, N-1324 Lysaker, Norway. Formerly at [3].
[3]IKU Petroleum Research, N-7034 Trondheim, Norway.

© 1996 European Association of Geoscientists & Engineers

suggested that the area of the interface between the air and the water is larger than expected due to the fact that the bubble surface is not perfectly smooth. An increase of the bubble area in the modelling, when mass transfer is included, leads to increased damping of the bubble oscillation.

The common feature in most of the suggested energy-loss mechanisms is that they are usually introduced as empirical functions and factors, in order to accommodate the synthetic signatures to the measured pressure pulses. Terms which might be significant for the energy-loss mechanisms in the Navier–Stokes equation have been omitted in the derivation of the equation describing the movement of the bubble wall. The simplest equation describing the motion of the bubble wall is the equation derived by Rayleigh (1917), known as the incompressible approximation. The approximation implies that the density of the water is constant and the speed of sound is infinite. This equation, however, contains no energy-loss mechanisms. In the acoustic approximation (Herring 1941), compressibility terms are introduced and the speed of sound in the liquid is a finite constant. Kirkwood and Bethe (1942) derived an equation in which the sound velocity in water is a function of the bubble motion. The theory given by Kirkwood and Bethe (1942) is the most commonly used theory for describing the behaviour of the bubble generated by an airgun. The computer-modelled signatures, calculated on the basis of the Kirkwood–Bethe (1942) theory, and a pressure distribution given by Gilmore (1952), are underdamped compared with measured signatures. A comparison of the above mentioned bubble models for different amplitudes, and their areas of validity, is given by Vokurka (1986). He concluded that the Gilmore adaptation of the Kirkwood–Bethe (1942) formulation remains irreplaceable in the studies of shock waves and strong pressure pulse propagations.

In order to investigate the surface of the bubble throughout the motion, and to detect turbulence in the vicinity of the bubble wall, high-speed photography of the bubble generated by a small airgun was performed. Possible scatterers inside the bubble can be discovered by illuminating the bubble with a concentrated laser beam. If the high-energy laser beam is scattered in the air volume, it is reasonable to assume that there exist particles inside the bubble that might originate from mass-transfer effects. Photographic snap-shots of the bubble with a pulsed laser as a flash have been recorded. Due to the short duration of the laser pulse (6–7 ns) and high energy output, this type of laser is very suitable to 'freeze' high-speed phenomena and gives sufficient light to expose film in an ordinary camera.

High-speed photography

In the experiment, an 850 litre tank filled with fresh water was used. The gun used was a BOLT 600B with a firing chamber of 1.6 cu.in., placed at 0.5 m depth, and having an operating pressure of 100 bar (1450 psi). During the high-speed photography, a HYCAM 16 mm camera with an available maximum framing rate

of 10 000 frames per second was used. The illumination was conventional white light, provided by four 800 W and six 500 W lamps. The available illumination was insufficient for making sharp pictures of the bubble surface, but lighting the gun towards the camera gave valuable information of the radial movement and silhouette of the bubble. The camera and the gun were triggered together and the camera was operated in different speed modes for obtaining the best photographs with the given light intensity. Photographs of the bubble recorded by high-speed cinematography are shown in Fig. 1. The film speed was 1000 frames per second.

It is also interesting to estimate the bubble radius and bubble-wall velocity from the individual frames and compare them with the modelled bubble radius and bubble-wall velocity for a 1.6 cu.in. gun. Bungenstock (1973) describes a similar experiment to ours, in which he used 2460 photographs per second to study the bubble generated by airguns. This paper includes an extensive study of many different source volumes and numerous photographs are presented. Johnston (1982) used high-speed film sequences of a Mod I 0.66 litre airgun fired at a depth of 1 m for comparison of theoretical and experimental bubble radii. By knowing the dimensions of the gun, and using the film exposed with a speed of 3000 frames per second, it is possible to determine roughly the velocity and radius as a function of time. The modelled signature is adapted to match a measured signature in the tank by using the theory outlined in the Appendix. The modelled and measured signatures are shown in Fig. 2a. The estimated bubble radius during the first period is shown, together with the modelled bubble radius in Fig. 2b. The radius is determined by assuming that outside each port a single bubble is formed, and that the total bubble volume consists of four bubbles merging into one. The result of the estimated velocity during the first bubble period is shown, together with a modelled velocity profile in Fig. 2c.

In order to obtain sharp photographs of the bubble and its surface, a light source of high intensity and short duration, and an ordinary camera, are required. Alternatively a continuous light source and a camera with a very high film speed could be used. An alternative would, of course, be a laser with a pulse repetition rate that could cope with the number of frames of a high-speed camera, triggering the laser and camera together, but this equipment is expensive and was not available. The best method, with the resources available, was to use a pulsed Nd:YAG laser as a flash. This laser has sufficient output energy to expose slides of 1000 ASA and the duration of the laser pulse is short enough to 'freeze' the movement of the bubble wall. The wavelength of this laser, when operated in double-frequency mode, is 532 nm (green light). The pulse duration is 6–7 ns and the output energy per pulse is approximately 100 mJ. In addition, green light is very suitable for transmission in water. The laser beam was expanded to cover the area of interest and the laser and the gun were triggered together. Snapshots of the bubble at different times could be made by adding a time delay to the laser. The drawback to this method is that it is not possible to make a continuous sequence of photographs of one bubble, hence only one photograph per bubble (i.e. shot) is

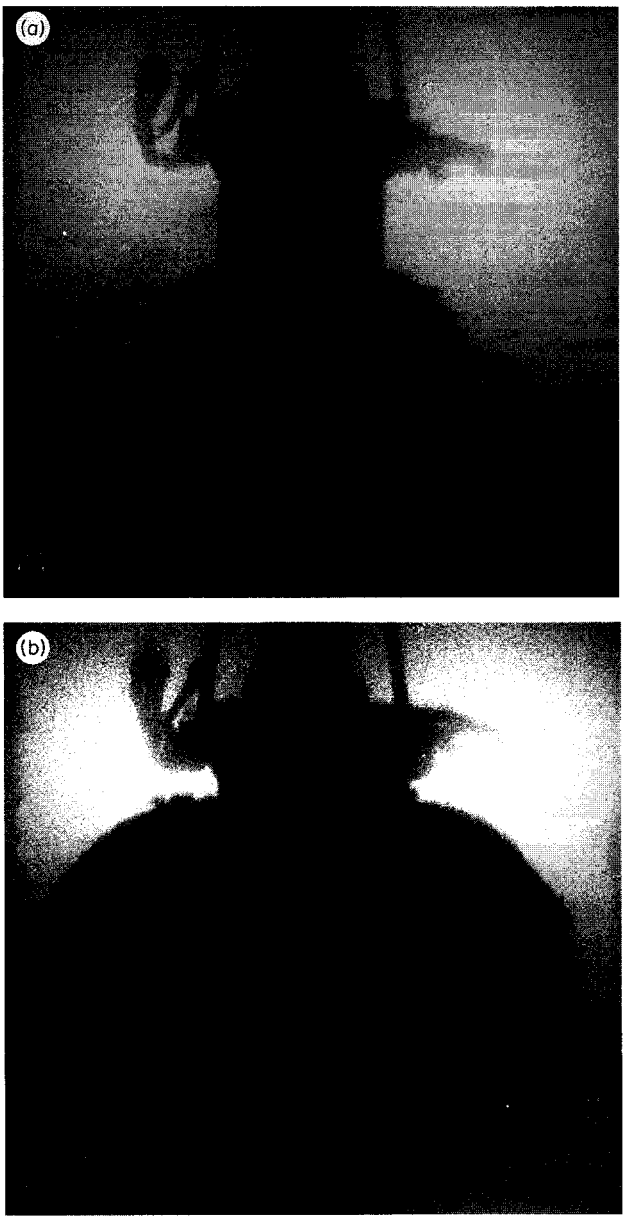


Figure 1. Photographs of the bubble recorded with a film speed of 1000 frames per second. The times for the frames are given from the time the air starts to escape from the ports and are: (a) 2 ms, (b) 11 ms, (c) 16 ms, (d) 25 ms.

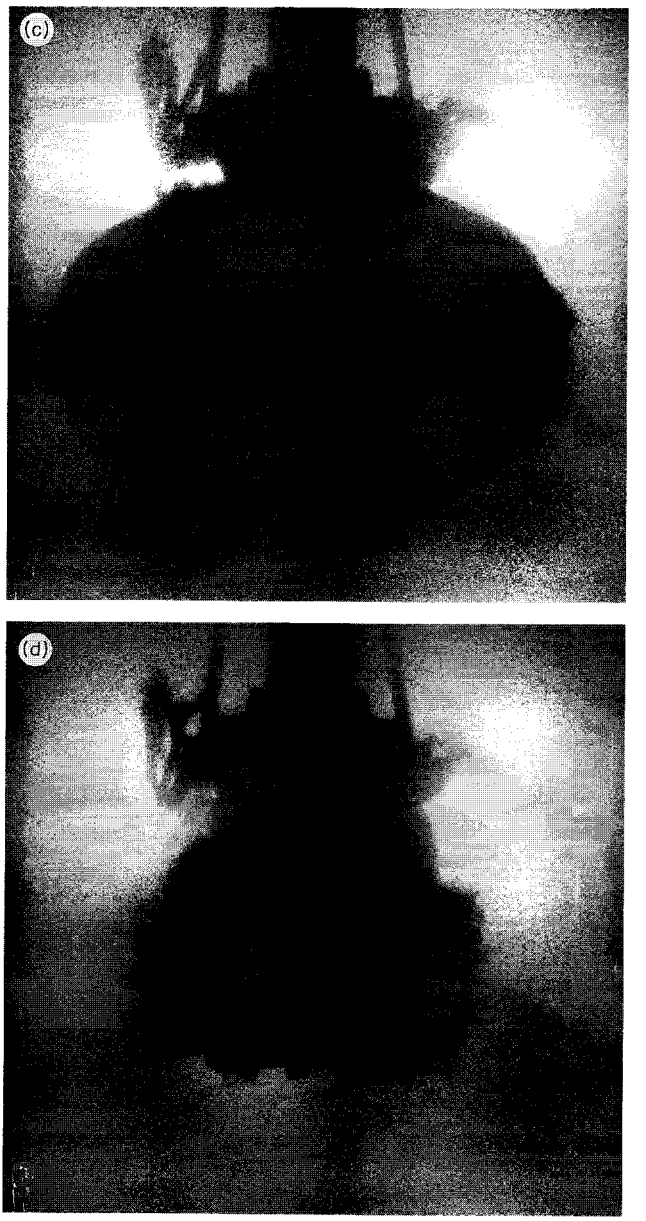
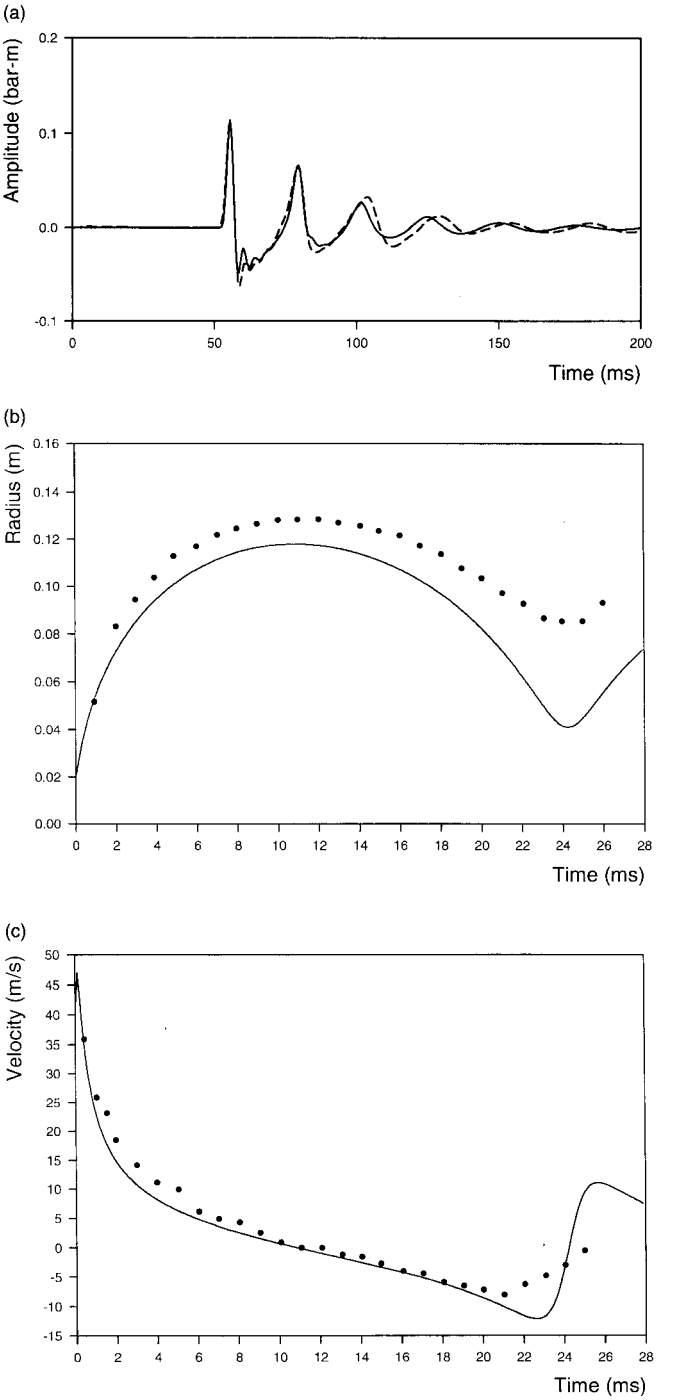


Figure 1. (Continued)


(a)
Amplitude (bar-m)
0.2
0.1
0.0
-0.1
0
50
100
150
200
Time (ms)
(b)
Radius (m)
0.16
0.14
0.12
0.10
0.08
0.06
0.04
0.02
0.00
0
2
4
6
8
10
12
14
16
18
20
22
24
26
28
Time (ms)
(c)
Velocity (m/s)
50
45
40
35
30
25
20
15
10
5
0
-5
-10
-15
0
2
4
6
8
10
12
14
16
18
20
22
24
26
28
Time (ms)

recorded. If the repeatability of the gun and bubble movement is good, which it is reasonable to assume, a time series of photographs of the bubble for study of the shape and surface can be recorded. Photographs of the bubble with a laser as a flash are shown in Fig. 3.

One of the main theoretical issues in airgun bubble dynamics is whether water vapour or water droplets exist inside the bubble. If the interior of the bubble consists of a mixture of air and water, this will influence the bubble dynamics and the physical processes that occur at the interface between the bubble and the surrounding water. A concentrated laser beam from the Nd:YAG laser was used to illuminate the bubble wall. In addition, the laser and the gun were triggered simultaneously, and the laser flash exposed slides in an ordinary camera equipped with a 100 mm lens. Photographs of the bubble at different times and from different directions are shown in Fig. 4.

Discussion

From the high-speed film, it can be seen that the bubble is defined best and has a relatively smooth surface during the first expansion. This has also been verified using holography during investigation of the bubble surface (Langhammer *et al.* 1995). The form of the four air jets is symmetrical during the first expansion and the bubble is approximately spherical at the first maximum. Figure 5 shows a sequence of pictures of the bubble photographed by a high-speed videocamera, placed above the tank, confirming that the air volume is approximately spherically symmetrical at the first maximum radius. When the bubble contracts, the surface becomes more irregular, and during the second oscillation the interface between the air and the water becomes highly irregular and chaotic. It can also be seen (Fig. 5) that, for this gun type, the air jets change direction when starting the second expansion. As the bubble oscillates the turbulence becomes more and more developed at the bubble wall. This turbulence has the effect of dispersing a small part of the gas in the bubble into the water.

From Fig. 2, it can be seen that there is a difference between the theoretical and the experimental bubble radii. Since the signature measured in the tank is influenced by the boundaries throughout the motion, damping coefficients were used in the Kirkwood–Bethe (1942) equation (see Appendix) in order to obtain a good match between modelled and measured signatures for the first period. The modelled bubble radius and bubble-wall velocity are obtained by assuming a perfectly spherical oscillating air volume. We assume that the main reason for the

Figure 2. (a) Modelled signature (solid line) and measured signature (dashed line) in the tank. Filter: 0-128 Hz (72 dB/oct) DFS V. (b) Bubble radius measured from the high-speed pictures (dots). Time interval between every chosen photograph is 1 ms. The solid line shows the modelled result. (c) Estimated bubble-wall velocity during the first bubble period from high-speed photographs (dots). The solid line shows the modelled result.

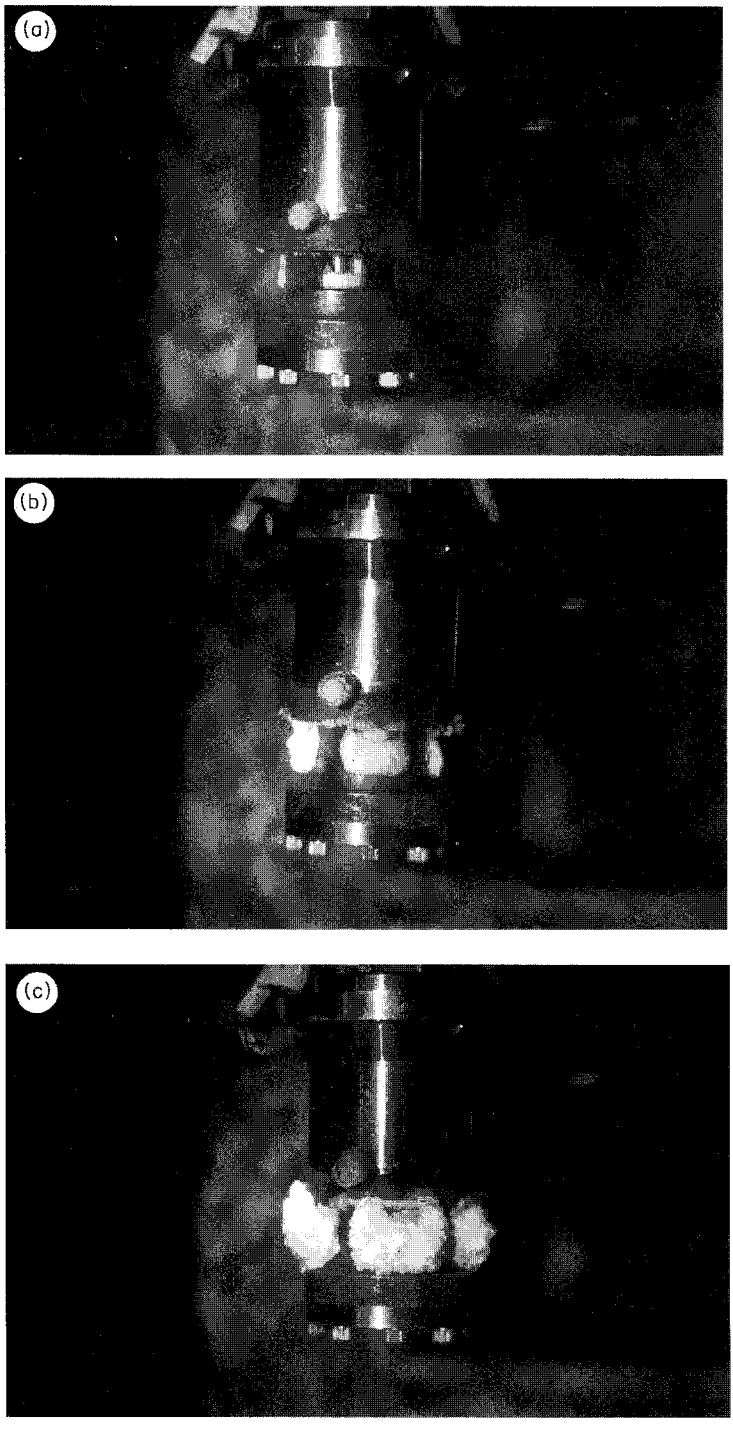


Figure 3. Photographs of the bubble at approximate times: (a) 0.2 ms, (b) 0.5 ms, (c) 1 ms, (d) 1.5 ms, (e) 7 ms, (f) 11 ms, (g) 16 ms, (h) 22 ms, (i) 25 ms, (j) 27 ms, (k) 30 ms, (l) 33 ms, after the gun starts releasing the air from the firing chamber.

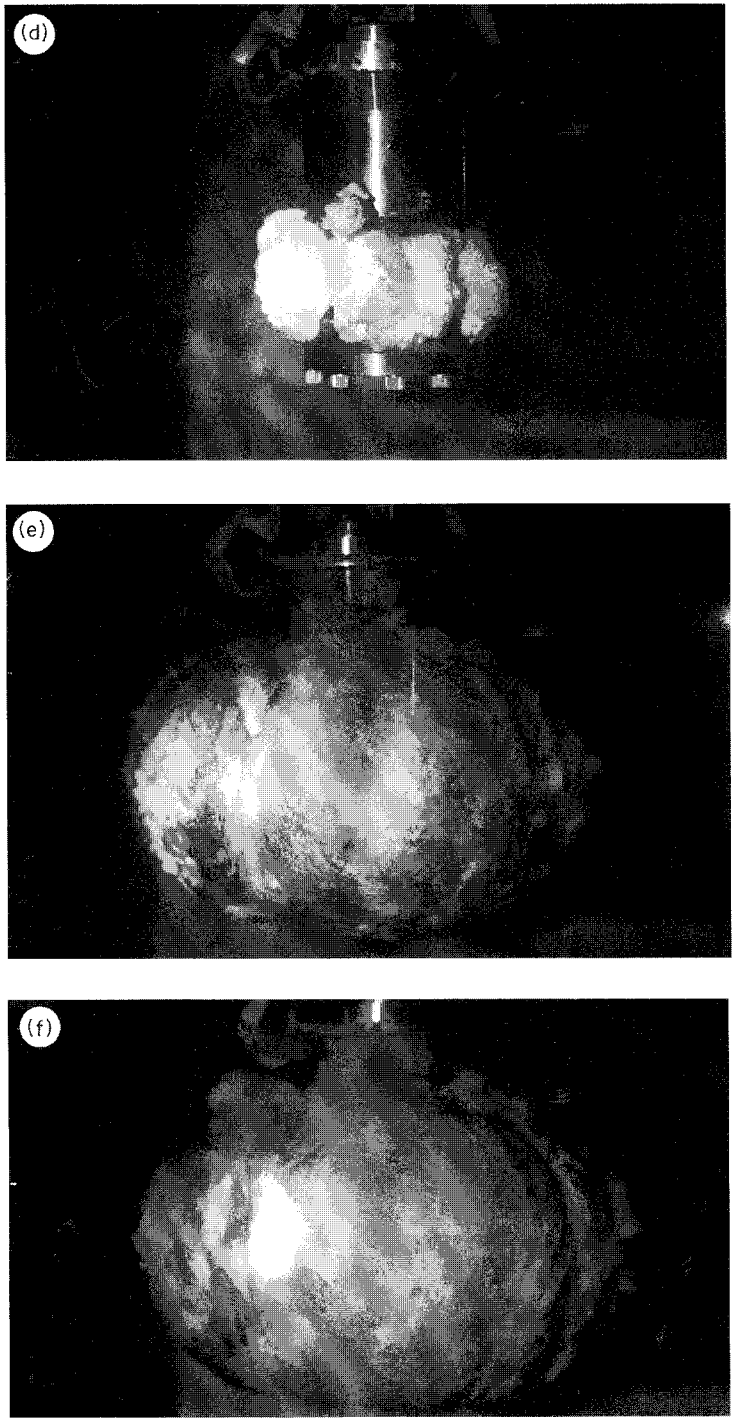


Figure 3. (Continued)

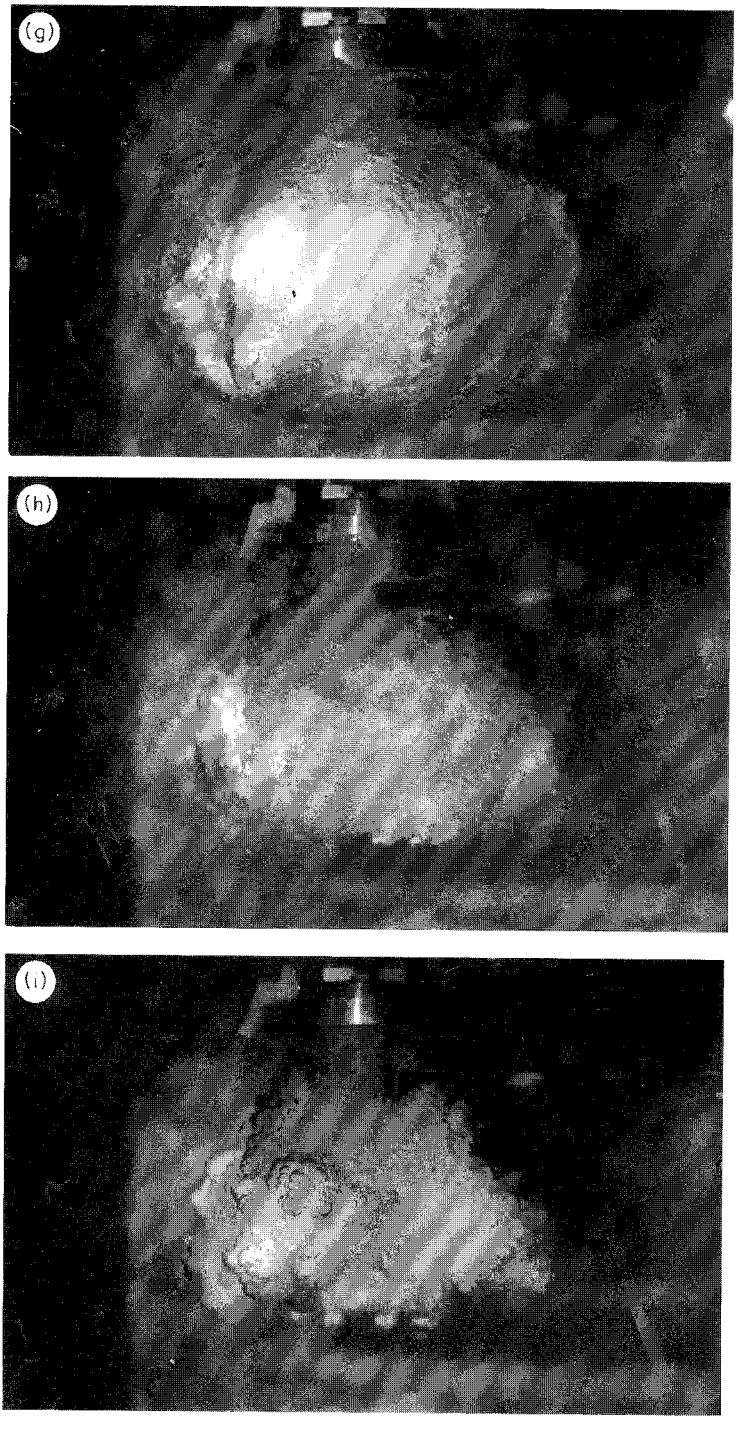


Figure 3. (Continued)

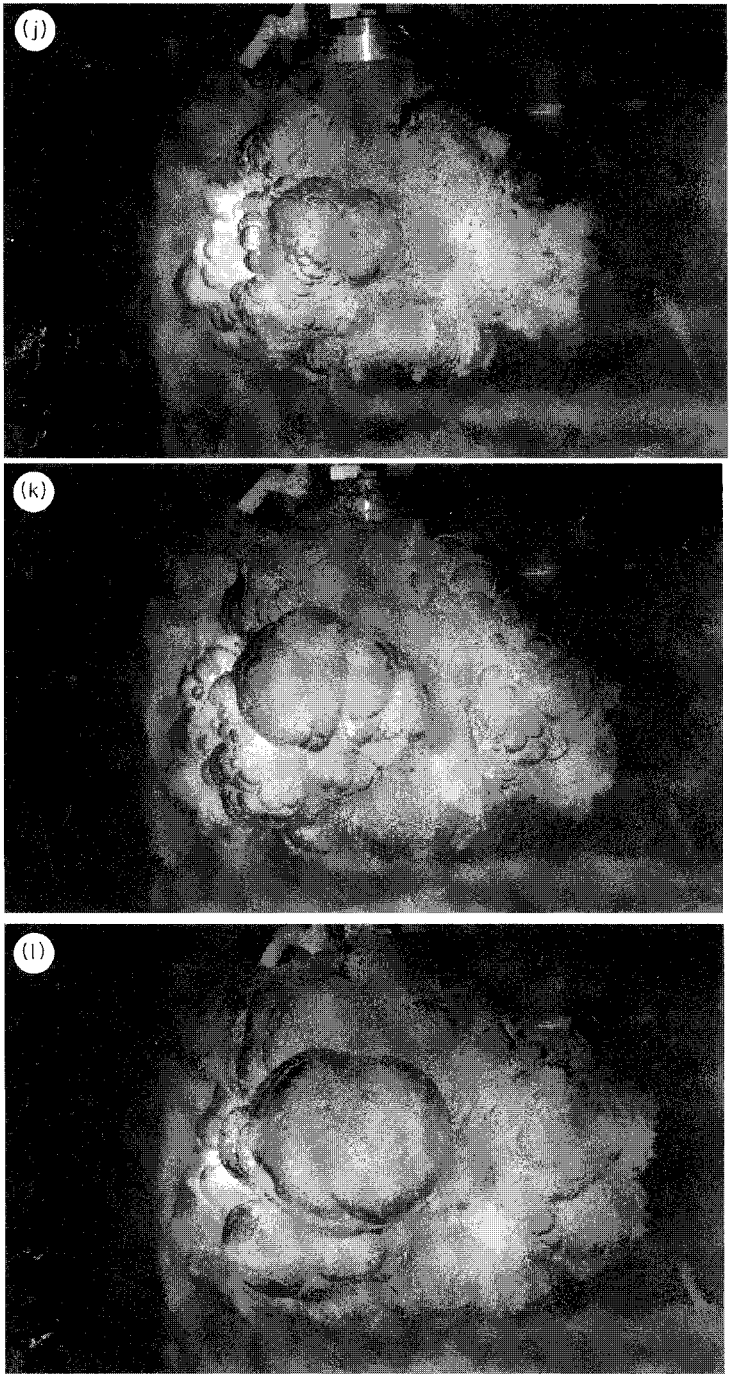
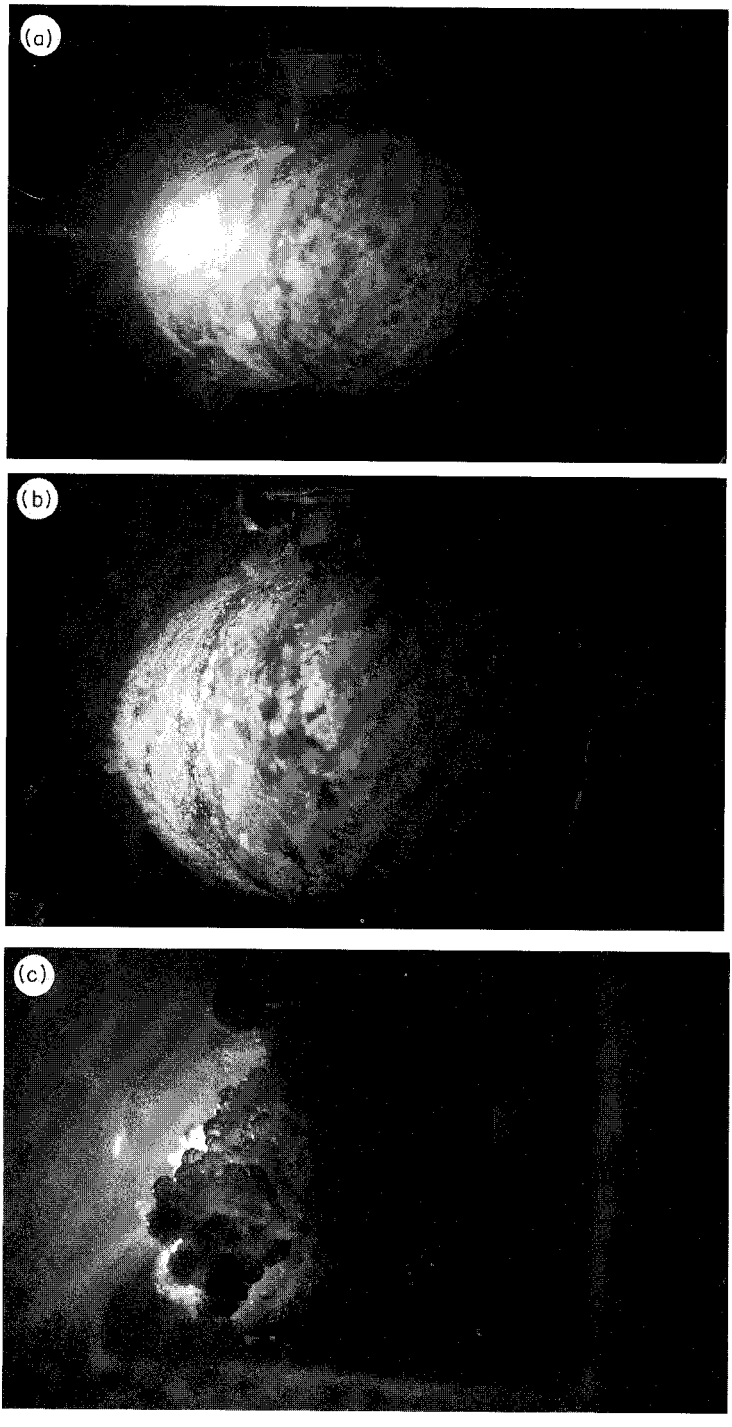


Figure 3. (Continued)


(a)
(b)
(c)

difference in radii is that the BOLT airgun with four ports actually creates four bubbles at the initial stage which merge into one bubble during the expansion. Also the presence of the gun causes the radius to be slightly larger than the corresponding modelled radius due to the fact that the gun occupies a volume that is filled by the bubble in the modelling situation. Correction for this at the maximum expansion decreases the effective radius of the air volume by about 0.5 cm compared with the value estimated from the high-speed film sequence. The presence of the gun body is assumed to influence the radius and bubble movement significantly at the minimum contraction. Johnston (1982) found agreement within 20% between theory (he used a different theory from that used here) and experiment for bubble radius during initial bubble growth. He was not able to obtain underwater film sequences beyond the first expansion due to murky water at the test location, which reduced the quality of the film. During the initial expansion, the agreement between theoretical and experimental results for the radius is within 9%. The bubble-wall velocity shows a good match during the expansion phase and a partial match during the contraction phase, but the highly non-spherical shape at the end of the first contraction phase introduces a significant mismatch between the modelled values and the values estimated from the high-speed film sequences.

Schulze-Gattermann (1972) found that the airgun body at the centre of the bubble has an effect on the frequency and the damping of the signature. Assuming the airgun body to be replaced by a concentric sphere inside the oscillating gas bubble, he found by modelling that the bubble time period decreased and the first secondary pressure pulse increased, compared with an isothermal modelled bubble where the gun is absent. For the adiabatic case, using the Kirkwood–Bethe (1942) equation, without any additional damping mechanisms or empirical terms, the modelled signature has a bubble time period that is far shorter than measured, and the secondary bubble oscillations have amplitudes that are much bigger than measured. The mismatch of the bubble period and damping, when comparing modelled and measured signatures, cannot be explained by corrections due to the presence of the gun. Energy-loss mechanisms, such as transfer of mass and heat and an increasing turbulence, are the most possible explanations of the mismatch between modelled and measured signatures.

Influence of gravity

On the film sequences it can be seen that the buoyancy has a negligible influence on the motion during the first bubble period. From the theory (Taylor 1942), it is

Figure 4. Photographs of the bubble from different directions and at different time instants when illuminating the bubble wall by a concentrated laser beam. (a) 6 ms (camera placed at 90° to the direction of the laser beam); (b) 11 ms (camera placed towards the laser beam); (c) 26 ms (camera placed towards the laser beam.)

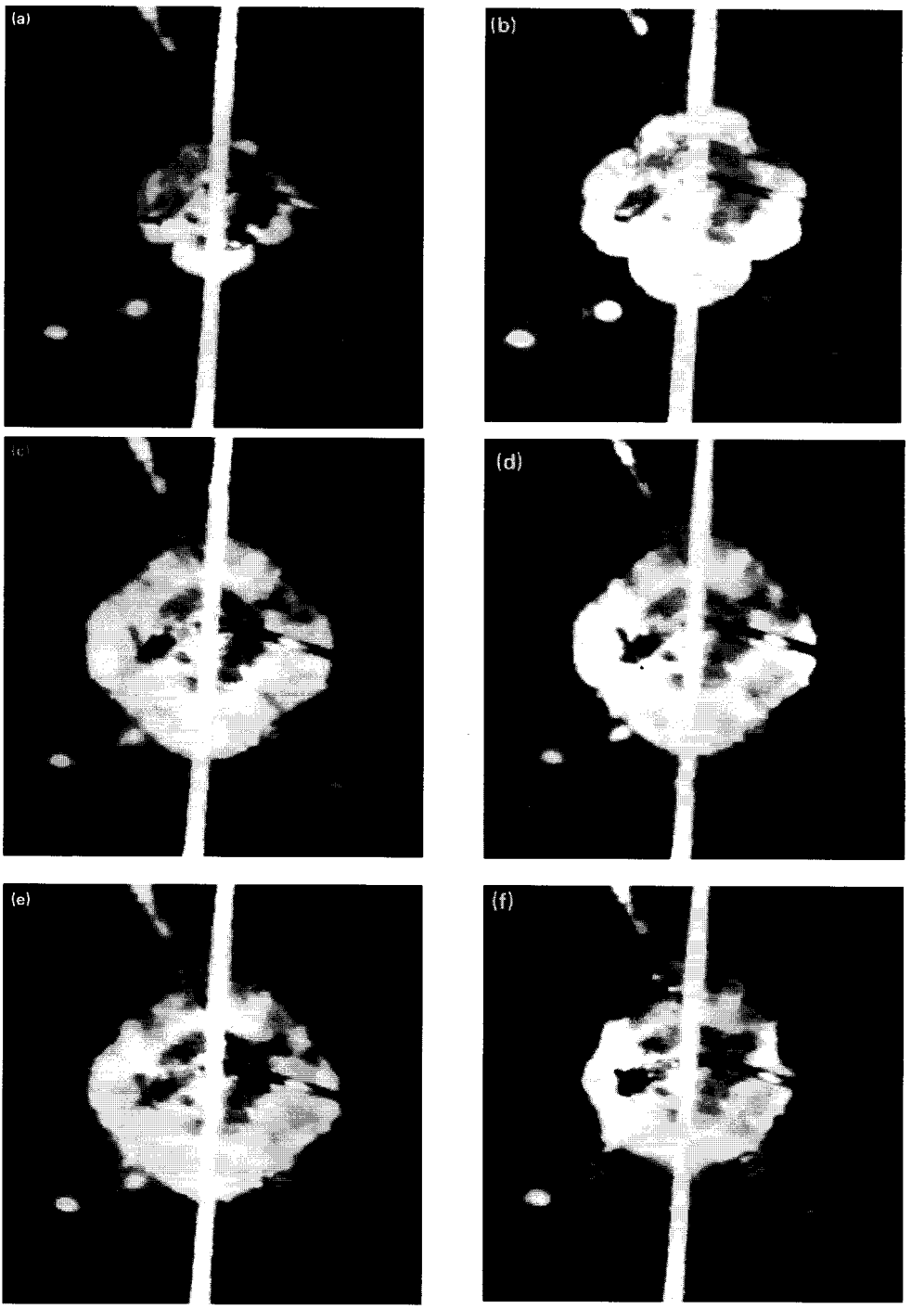


Figure 5. Photographs of the bubble from a location above the tank using a high-speed videocamera with a rate of 1000 frames per second. The time intervals for the photographs after the gun starts to release the air into the water are: (a) 2 ms, (b) 4 ms, (c) 9 ms, (d) 11 ms, (e) 13 ms, (f) 18 ms, (g) 21 ms, (h) 24 ms, (i) 26 ms, (j) 29 ms, (k) 39 ms, (l) 55 ms.

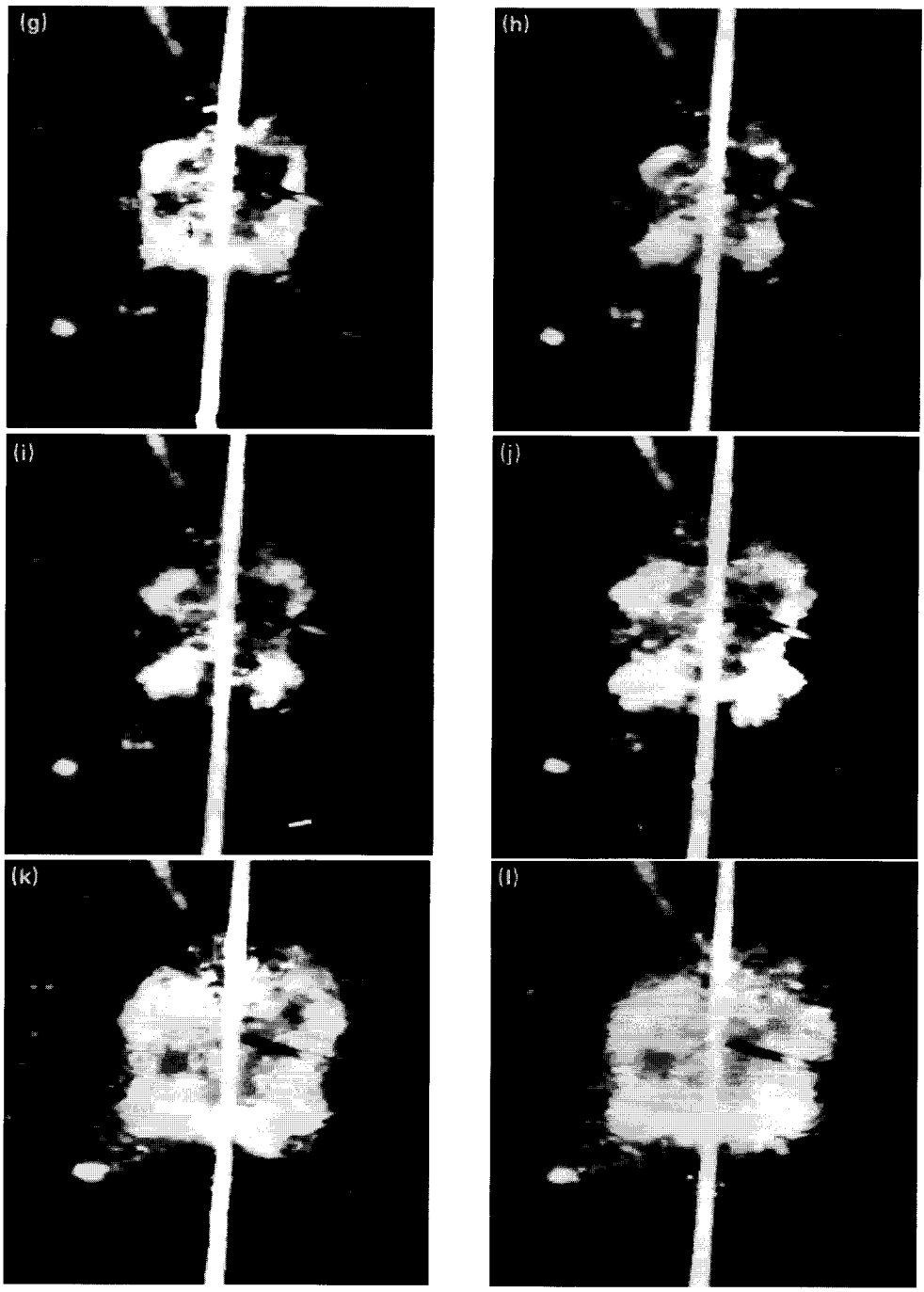


Figure 5. (Continued)

calculated that during the first expansion phase of the bubble motion there is very little vertical migration, but near the minimum radius the upward migration becomes more appreciable. Herring (1941) analysed the form of the bubble surface when gravity is included in the equation of motion. To a first approximation, the bubble remains spherical, but this approximation becomes more and more crude in later stages. During the period when the gravity effect is small, its only influence is to displace the bubble vertically without perturbation of the shape. A first-order correction to the radius vector is an equal upward displacement of all points of the surface. The velocity U_d of this displacement is given by (Herring 1941; Taylor 1942)

$$U_d = \frac{2g}{R^3}\int_0^t R^3 dt, \tag{1}$$

where g is the gravity and R is the bubble radius. This upward velocity increases with time and in particular when the radius becomes small in the contraction phase due to the factor $1/R^3$. Implementation of (1) in the computer modelling gives a curve of the vertical displacement of the bubble as shown in Fig. 6. From the curve it can be seen that the bubble centre migrates about 1.5 cm during the first bubble period. The corresponding estimated vertical displacement obtained from the high-speed filming is about 1 cm. The displacement of the bubble relative to the gun

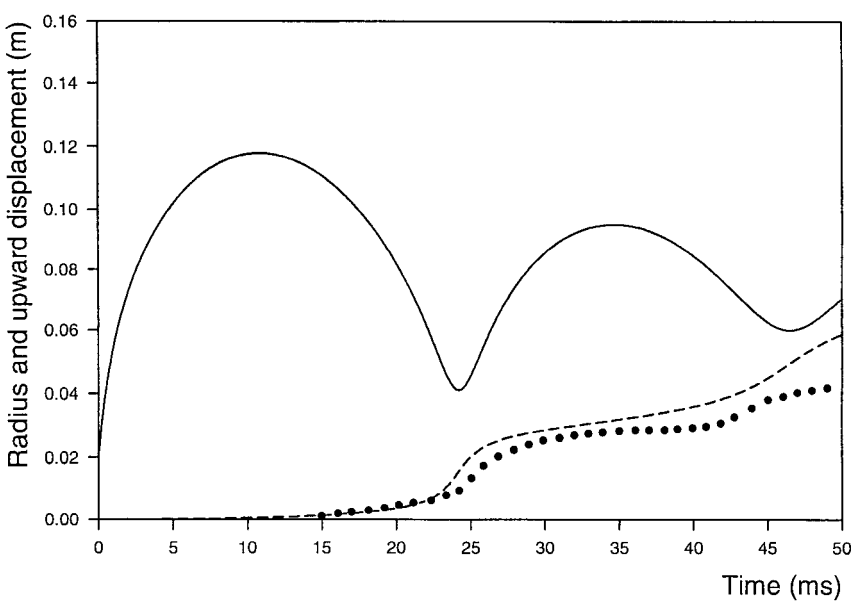


Figure 6. Modelled bubble radius (solid line) and modelled upward displacement (dashed line). The dots mark the upward displacement of the bubble centre estimated from high-speed filming.

within this time interval can therefore be neglected. The high-speed film sequences show that the upward displacement of the bubble during the first two bubble time periods is of the same order as that obtained from modelling, but the approximation given by (1) becomes more crude at the later stages of the oscillation. The theoretical calculations have not taken into account the movement of the free surface which also introduces a difference between the modelled migration and the migration estimated from high-speed recordings. It is not possible to determine the upward displacement of the bubble centre accurately from photographs because the bubble is elongated in the vertical direction at the first minimum, and this makes it difficult to predict the bubble centre. Schulze-Gattermann (1972) also concluded from high-speed recordings that the upward distance travelled by the bubble centre during the first oscillation is negligible compared with the dimensions of the gun.

Influence of the boundaries

Since the gun is fired in a small tank, it is assumed that the bubble time period for the gun fired in the tank does not coincide exactly with the bubble time period for the same gun fired in open sea conditions. The mass flow of water is disturbed by the free surface and the walls of the tank. For comparison of the signatures measured in the tank, signatures have been recorded in a larger tank (360 m^3) and in a free field. The two tank signatures and the free-field signature are shown in Fig. 7. As pointed out earlier (Langhammer and Landrø 1993), the water temperature has an influence on the signature regarding the primary-to-bubble

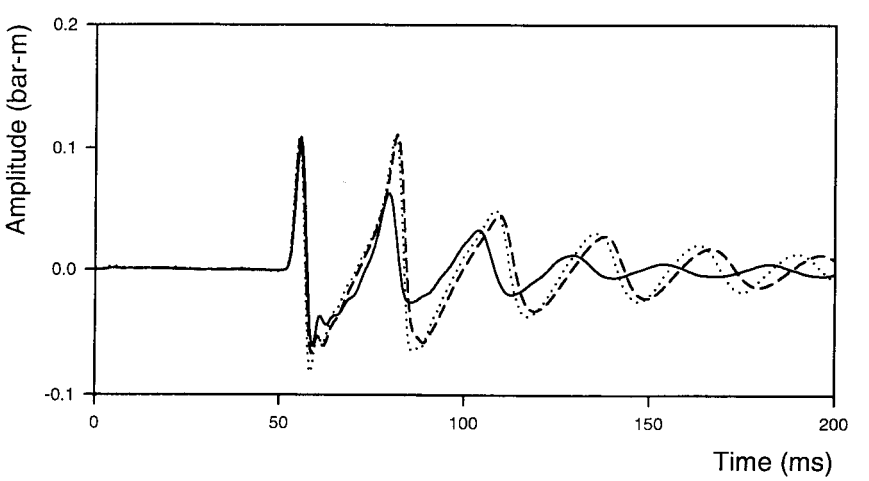


Figure 7. Measured near-field signatures from the 1.6 cu.in. gun in the 0.85 m^3 tank (solid line), in the 360 m^3 tank (dashed line), and in a free field (dotted line). Filter: 0-128 Hz (72 dB/oct) DFS V.

ratio and the bubble time period. The water temperature in the 0.85 m^3 tank, when recording the pressure pulse, was approximately 7°C, the water temperature in the 360 m^3 tank was approximately 18°C and the seawater temperature was approximately 12°C. The bubble peak and the bubble time period for the larger tank and the free-field signature exceed the values of the signature measured in the tank. The difference between the small-tank signature and the free-field signature is too large to be explained by the difference in water temperature. The difference in rebound when firing the gun in a small tank and in a free field is a more plausible explanation. But the difference in bubble time period between the larger tank and the free-field measurement is mainly due to temperature difference. The salt in the seawater is assumed to have no observable influence on the measurements compared to fresh-water measurements.

The bubble in the small tank does not undergo the same dramatic collapse as the bubble in the free field, where a much larger amount of water is involved in the bubble movement. The confining walls contribute to an increased non-linear fluid flow around the bubble compared to a gun fired in a free field. This effect yields a contribution when the bubble starts to collapse after the first expansion and increases successively throughout the motion of the bubble.

Laser scattering

From the photographs in Fig. 4, where the concentrated laser beam was used as a light source, it can be seen that part of the incoming beam is reflected off the bubble surface. However, some of the light is transmitted through the bubble wall and illuminates the interior of the bubble. This can in particular be observed in Fig. 4b, where the gun is placed between the laser and the camera, hence the laser beam is propagating straight towards the camera. All the photographs show that the laser beam is scattered in the interior of the bubble, hence it is reasonable to assume that the light is multiply scattered by small particles. The photographs from high-speed cinematography, where the silhouette of the bubble has been investigated, show that the bubble is opaque even at the edge. This indicates that the bubble from an airgun might be a mixture of air and fog, or that it contains a great number of water droplets. The fog and droplets may arise either from mass-transfer mechanisms such as condensation and evaporation at the bubble wall (Ziolkowski 1982; Laws *et al.* 1990; Langhammer and Landrø 1993) or by an injection of water when the air is rapidly transferred from the gun into the water. Most of the water spray is assumed to be injected into the bubble just after the throttling starts and may last until the bubble radius reaches its first maximum. When the bubble continues to oscillate the amount of spray decreases due to the decreased bubble-wall velocity. Finally, the water droplets are assumed to migrate to the lower part of the bubble due to gravity and are absorbed by the air/water interface.

Conclusions

High-speed cinematography of the bubble generated by a 1.6 cu.in. BOLT airgun in a small tank has been performed with the purpose of investigating the shape, surface, turbulence and different physical processes for the airgun bubble. During the first expansion, the bubble surface is relatively smooth and the movement of the surrounding fluid is mostly radial. As the bubble contracts and continues to oscillate, the surface becomes much more irregular and turbulence develops. Bubble-wall velocity and bubble radius are estimated from photographs and compared with modelled results. From a light-scattering experiment, it is found that the bubble is a strong scattering medium for light. Laser light is multiply scattered in the interior of the bubble, and the bubble acts as an effective obstacle to light. This can be explained by the presence of a large number of scatterers such as water droplets, or fog, hence the bubble might consist of a mixture of air and water. This mixture may arise from either mass transfer processes such as evaporation and condensation, or water spray injected into the bubble during the expansion. Water inside the bubble will also increase the specific heat capacity considerably. This influences the bubble motion, and hence the output pressure waveform, which might explain why modelled signatures do not match measured signatures from airguns.

Acknowledgements

The financial support from the VISTA/STATOIL research program is highly appreciated. We thank Tor Øivind Ask of Marintek A/S for help during the high-speed filming of the bubble and Irene Vik of the Norwegian Institute of Technology (NTH) for laser expertise and photography assistance. The two anonymous reviewers are thanked for valuable comments and suggestions for improvement of the manuscript. Finally, we thank Eivind Berg of STATOIL for support in this project.

References

Bungenstock H. 1973. *Zur analyse und beeinflussung von seismischen signalen, erzeugt durch pneumatische schallquellen.* Geologisches Jahrbuch E1, Hannover.

Gilmore F.R. 1952. The growth or collapse of a spherical bubble in a viscous compressible liquid. Report No. 26-4. Hydrodynamics Laboratory, CALTEC, Pasadena, California.

Herring C. 1941. Theory of the pulsations of the gas bubble produced by an underwater explosion. OSRD Report No. 236.

Johnston R.C. 1982. Development of more efficient airgun arrays: theory and experiment. *Geophysical Prospecting* **30**, 752–773.

Kirkwood R.C. and Bethe H.A. 1942. OSRD Report No. 588.

Landrø M. and Sollie R. 1992. Source signature determination by inversion. *Geophysics* **57**, 1633–1640.

Langhammer J., Graciet S., Vik I., Espeland M. and Løkberg O.J. 1995. Holographic studies of the bubble generated by a seismic air gun. *Journal of the Acoustical Society of America* **97**, 362–369.

Langhammer J. and Landrø M. 1993. Temperature effects on airgun signatures. *Geophysical Prospecting* **41**, 737–750.

Laws R.M., Hatton L. and Haartsen M. 1990. Computer modelling of clustered airguns. *First Break* **8**, 331–338.

Rayleigh O.M. 1917. On the pressure developed in a liquid during the collapse of a spherical cavity. *Philosophical Magazine* **34**, 94–98.

Schulze-Gattermann R. 1972. Physical aspects of the "airpulser" as a seismic energy source. *Geophysical Prospecting* **20**, 155–192.

Taylor G.I. 1942. Vertical motion of a spherical bubble and the pressure surrounding it. *Underwater Explosion Research* **2**, 1950. Office of Naval Research, Dept. of the Navy.

Vokurka K. 1986. Comparison of Rayleigh's, Herring's and Gilmore's models of gas bubbles. *Acustica* **59**, 214–219.

Ziolkowski A. 1970. A method for calculating the output pressure waveform from an airgun. *Geophysical Journal of the Royal Astronomical Society* **21**, 137–161.

Ziolkowski A. 1982. An airgun model which includes heat transfer and bubble interactions. 52nd SEG meeting, Dallas, Expanded Abstracts, 187–189.

Ziolkowski A. 1990. Airgun array modelling theory. 52nd EAEG meeting, Copenhagen, Expanded Abstracts, 10–11.

Ziolkowski A. and Metselaar G. 1984. The pressure wavefield of an airgun array. 54th SEG meeting, Atlanta, Expanded Abstracts, 274–276.

Appendix

Computer modelling

In the modelling a damped Kirkwood–Bethe equation for describing the motion of the bubble was used (Kirkwood and Bethe 1942; Landrø and Sollie 1992), given by

$$\ddot{R}=\frac{H\left(1+\frac{\dot{R}}{C}\right)-\frac{3}{2}\dot{R}^2\left(1-\frac{\dot{R}}{3C}\right)+\dot{H}\frac{R}{C}\left(1-\frac{\dot{R}}{C}\right)-\alpha\dot{R}+\beta\dot{R}^2}{R\left(1-\frac{\dot{R}}{C}\right)} \qquad \text{(A1)}$$

where R is the bubble radius, C is the velocity of sound in water and H is the enthalpy at the bubble wall. The parameter α is a damping constant and β is an additional empirical factor which mainly influences the bubble time period ($\alpha = 0$ and $\beta = 0$ correspond to a 'true' Kirkwood–Bethe equation). The two parameters are evaluated in order to give a better match between the measured and the modelled signatures. For modelling the tank signature from the 1.6 cu.in. gun, α

and β were given the values 4.0 and 0.34 respectively. The temperature change inside the bubble is given by the equation (Landrø and Sollie 1992)

$$\dot{T} = \frac{R_g T\dot{m} - p\dot{V}}{mc_v} \tag{A2}$$

where R_g is the ideal gas constant, p is the pressure inside the bubble, V is the bubble volume, m is the mass of air and c_v is the specific heat capacity. A simple mass injection process has also been included in the modelling since the damping factors α and β cannot alone provide a sufficient match between the measured and modelled signatures. It must be noted that any mass transfer process has a large influence on the rate of change of the temperature, and hence on the modelled signature.